Online supplement

Hypersonic Weapons: Vulnerability to Missile Defenses and Comparison to MaRVs

David Wright & Cameron L. Tracy (2023) Hypersonic Weapons: Vulnerability to Missile Defenses and Comparison to MaRVs, Science & Global Security, DOI: 10.1080/08929882.2023.2270292

Appendices A, B, C, and D

David Wright[1] and Cameron L. Tracy[2]

Table of Contents

[1] David Wright, dcwright@mit.edu, Visiting Scholar, Laboratory for Nuclear Security and Policy, Department of Nuclear Science and Engineering, MIT

[2] Research Scholar, Center for International Security and Cooperation (CISAC), Freeman Spogli Institute for International Studies, Stanford University

Appendix A: Coordinate System Used in "Modelling the Performance of Hypersonic Boost-Glide Missiles"

Our previous paper uses simplified equations of motion (Equations (1) – (6) in that article) that are appropriate for the quantities we calculated.1 In the corresponding coordinate system, Ψ and Ω are the down-range and cross-range angles, with distances measured along great circles so that Ψre is the range and Ωre is the cross-range distance.2 The advantage of these coordinates for our calculation is that the velocity angle κ has a simple physical interpretation as the direction of motion relative to the down-range direction.

Also, as we discuss below, using the full set of equations in spherical coordinates requires an additional set of equations to determine what an observer on the Earth would consider range and cross-range distances, due to the nature of spherical coordinates near the poles.

The full set of equations of motion in spherical coordinates (ignoring Earth's rotation), as given in reference 21 of the original paper, would replace Equations (3) – (5) in our paper with these equations:

$$\frac{d\eta}{dt} = \left(L/D\right)\left(\frac{C_d A}{2m}\right)\frac{\rho v \sin\sigma}{\cos\gamma} - \frac{v\, tan\theta\, \cos\gamma \sin\eta}{r_e + h} \quad (3')$$

$$\frac{d\theta}{dt} = \frac{v\cos\gamma\cos\eta}{r_e + h} \quad (4')$$

$$\frac{d\phi}{dt} = \frac{v\cos\gamma\sin\eta}{(r_e + h)\cos\theta} \quad (5')$$

where θ and ϕ are geographic latitude and longitude coordinates, and η is the heading angle of the velocity vector measured from north. The origin of the coordinate system, and the launch location of the vehicle, is a point on the equator with zero latitude and longitude. The vehicle is assumed to be launched north along the line of zero longitude.

These equations differ from (3) and (5) by the appearance of the second term in (3') and the factor of $\cos\theta$ in (5'). (The appearance of radius r_e rather than $r = r_e+h$ in Equations (4) and (5) was a typo in the original paper; our calculations used the correct version.)

Using Equations (3') – (5') requires new equations for down-range and cross-range distances. These distances (measured along great circles) for a vehicle at a point with latitude and longitude (θ, ϕ) are given by:

$$crossrange = \varepsilon r_e \quad (A1)$$

$$range = r_e\, cos^{-1}\left(\frac{\cos\theta\cos\phi}{\cos\varepsilon}\right) \quad (A2)$$

where

$$cos^2\varepsilon = \left(1 + sin^2\theta + cos^2\theta\cos(2\phi)\right)/2 \quad (A3)$$

The geometrical difference between the two coordinate systems and a derivation of Equations (A1) – (A3) is discussed below.

Both sets of equations give identical results for flight purely in the down-range direction. They also give differences of only a few percent or less in range and cross-range for the maneuvering calculations presented in the paper, the results of which are shown in Figures 6 and 14 of that paper.

Calculating Range and Cross-range in Different Coordinate Systems

Assume a vehicle begins flying at the origin and at some time is located at a point *P*. Figure A1 shows in blue how *P*'s coordinates (θ, ϕ) are defined in terms of latitude and longitude. Flight begins in the north direction, so the longitude = 0 circle defines the range direction.

It is important to note that given a point *P*, there are (at least) two ways to associate a point on the longitude = 0 line with point *P*, and to define the "cross-range" distance between *P* and the longitude = 0 line:

(1) Draw a latitude circle through *P* (that circle is defined by the intersection of the sphere with a plane parallel to the equatorial plane). Define point *A* as where that latitude line crosses the longitude = 0 line (see Figure A1). θ is the angle between the x-axis and a radial line from the center of the sphere to point *A*. In this case, the distance from *P* to *A* along the latitude line is $\phi \, Re \cos\theta$, but that is not what you would call the "distance between *P* and *A*" which would instead be defined along a geodesic of the sphere, that is, along a great circle.

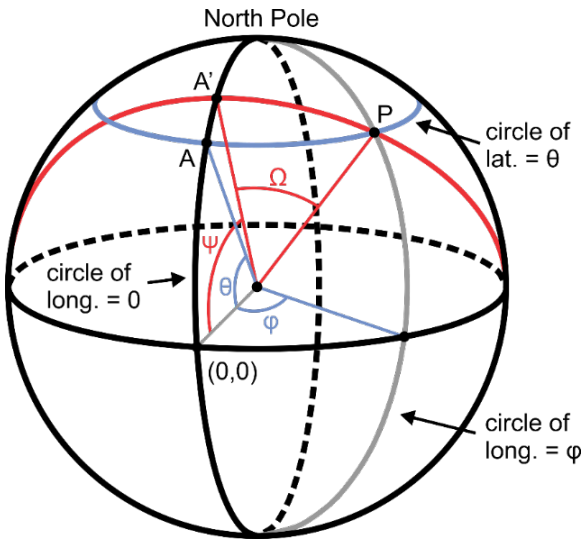

Figure A1. This figure shows two ways of assigning coordinates to a point P. Standard spherical coordinates for P are shown in blue. The vehicle is launched at (0,0) and the "range" direction is along the circle of longitude = 0 toward the north pole. The "cross-range" distance to P is the distance measured along the red great circle to A'.

(2) The correct way to associate range and cross-range distances with P is to draw a great circle through P that is perpendicular to the longitude = 0 line; this is shown in red in Figure A1. It crosses the longitude = 0 line at the point A'. The distance from the origin to A' is what an observer on the Earth would define as the "range" of a vehicle that had reached P, since the "cross-range" distance to P would be measured along a great circle passing through A' and P. The associated angles in this case, Ψ and Ω, are shown in red.

Figure A1 shows that Ψ is always larger than θ, although near the equator the difference is small.

Figure A2 illustrates the difference between θ and Ψ in an illustrative case. This figure is looking down on the north pole; the vehicle is launched from the equator and is passing by the pole on the red trajectory. It is clear that what we would call the "range angle" (Ψ) is 90 degrees, but in this case the spherical-coordinate angle θ never gets larger than 85 degrees.

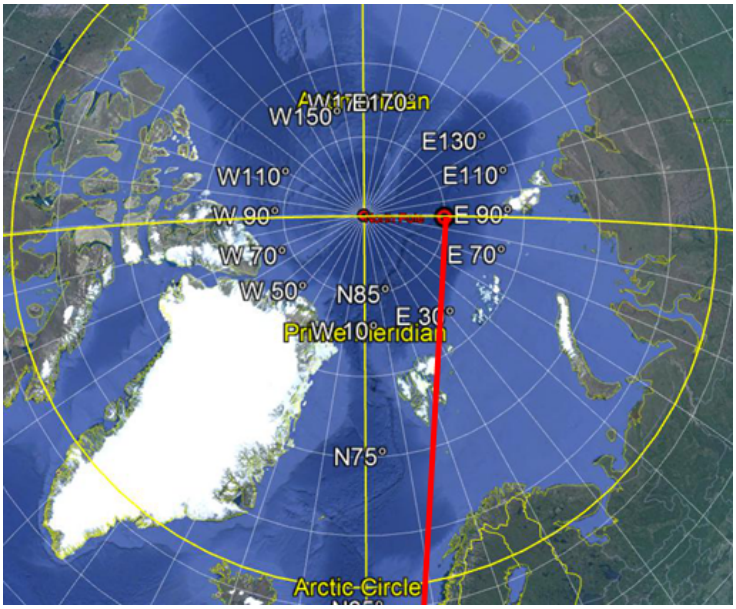

Figure A2. This figure shows a view from above the north pole of a vehicle launched from the origin; the trajectory is shown in red.

Derivation of Equations for Range and Cross-range from Spherical Coordinates

Figure A1 shows that the spherical coordinates angles θ and ϕ do not directly give the range and cross-range distances to a point P. This section derives equations for range and cross-range from those variables.

Consider a point at (latitude, longitude) = (θ,ϕ) (see Figure A3).

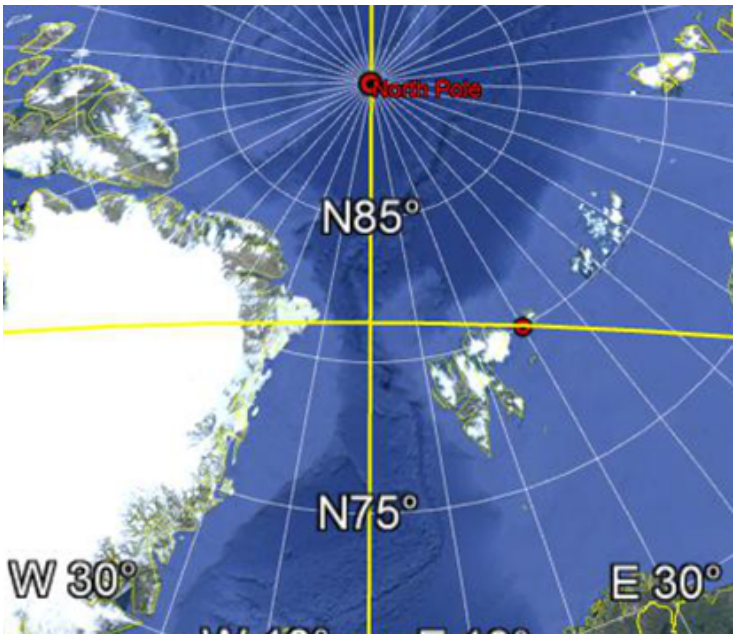

Figure A3: Consider the point shown in red at (N80, E30). The cross-range distance to the point is measured from the latitude = 0 line along a great circle, show as the horizontal yellow curve. Note that the distance measured along a line of latitude is a fraction $\phi/2\pi$ of the circumference of a circle at latitude θ, which is $2\pi\, r_e \cos\theta$. So this distance is $\phi\, r_e \cos\theta$.

The cross-range distance is measured along a great circle through the point, and can be found using spherical geometry:

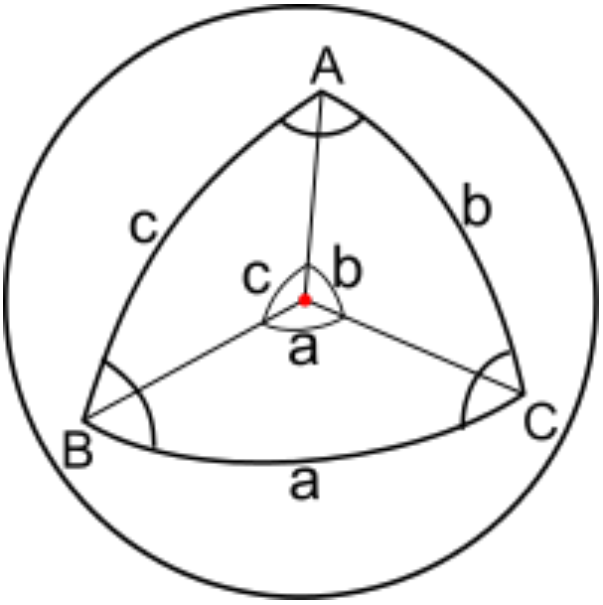

Figure A4: This figure assumes a unit sphere. In general the length of the arc subtended by the angle *a* will be *ar*, where *r* is the radius of the sphere. Here *A* is the angle between the arcs *AB* and *AC*, and *a* is the angle in the horizontal plane containing points *B* and *C*.

Consider a spherical triangle, with sides made of segments of great circles, as in Figure A4. Take *A* to be at the north pole, and *B* and *C* to be the points *(θ, ±ϕ)*. The angle *a* is 2*ϕ*, and angles *b* and *c* are (90 - *θ*).

The spherical law of cosines:[3]

$$\cos a = \cos b \cos c + \sin b \sin c \cos A \qquad (A5)$$

gives:

$$\cos a = sin^2\theta + cos^2\theta\cos(2\phi) \qquad (A6)$$

The cross-range is half the length of the great circle segment connecting b and c, which can be found from Equation (C6) as:

$$Crossrange = \frac{a}{2} r_e \qquad (A7)$$

The range angle corresponding to a point with (latitude, longitude) = *(θ,ϕ)* can be found in a similar way. Consider the line of longitude = 0, which bisects the angle *A* and the length *a* in Figure A4; this line is shown in red in Figure A5, which is the black triangle is that of Figure A4 with the points relabeled. The point where this line intersects the horizontal arc is labelled *F*. The range angle will be given by 90 – *e*, where *e* is the angle between the radial vectors from the center of the sphere to the points D and F.

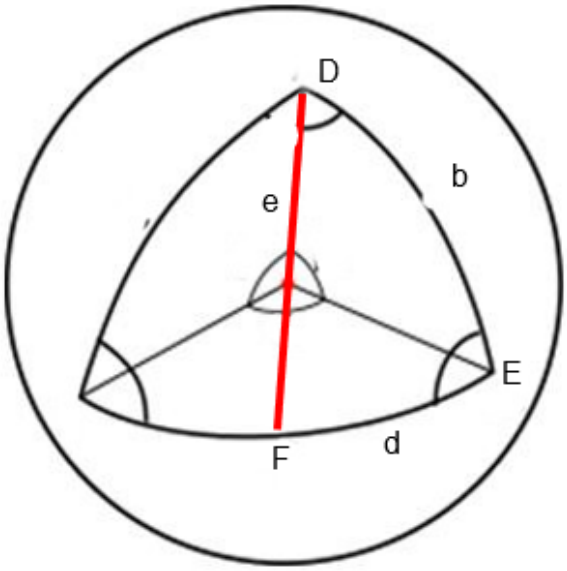

Figure A5. This figure shows the triangle from Figure A4 with the point relabeled. The red arc connecting *D* and *F* bisects the angle at *A* in the previous figure.

The angle $D = A/2 = \phi$, and the length $d = a/2\ r_e$, where a was calculated above.

From the spherical law of sines:[4]

$$\frac{\sin D}{\sin d} = \frac{\sin E}{\sin e} \qquad (A8)$$

so that

$$\sin e = \sin E \ \frac{\sin d}{\sin D} \qquad (A9)$$

From Figure A5:

$$\frac{\sin A}{\sin a} = \frac{\sin C}{\sin c} = \frac{\sin E}{\sin c} \qquad (A10)$$

where the last equality comes from the fact that angles C and E are the same in the two cases.

Combining these gives:

$$\sin e = \left(\frac{\sin\frac{a}{2}}{\sin a}\right)\left(\frac{\sin 2\phi}{\sin\phi}\right)\cos\Psi = \frac{\cos\phi\cos\theta}{\cos\frac{a}{2}} \qquad (A11)$$

or

$$\sin e = \frac{\cos\phi\cos\theta}{\left(\frac{1+\cos a}{2}\right)^{1/2}} \qquad (A12)$$

where *cos a* is given by Equation (A6). The range is then given by:

$$Range = \left(\frac{\pi}{2} - e\right) r_e \qquad (A13)$$

So for a point with (latitude, longitude) = *(θ, ϕ),* the range and cross-range distances are given by Equations (A7) and (A13).

Letting $\varepsilon = a/2$, so that it is the cross-range angle, these equations can be written in the alternate form given in Equations (A1) – (A3).

Appendix B: Implications of Increasing *L/D* and *β*

The parameters that determine the most important aerodynamic properties of a vehicle are its lift and drag coefficients, C_L and C_D, respectively. These are typically discussed in terms of the lift-to-drag ratio, $L/D = C_L/C_D$, and ballistic coefficient, $\beta = m/(C_D A)$, where A is a reference area of the vehicle.

L/D is the key parameter governing the range of a BGV, for reasons discussed below. While *L/D* for a subsonic aircraft can be in the range of 15 to 20, the values for hypersonic gliders are much lower; as noted in the text, *L/D* for the BGVs the United States is developing appear to be less than three.

It is useful to ask to what extent future BGVs might use designs and materials that could significantly increase *L/D*, and to what extent increasing *L/D* might significantly improve the military capabilities of these weapons.

Studies show that in principle it may be possible to increase the *L/D* values of hypersonic vehicles to six or higher using waverider designs described in the text.[5] Increasing *L/D* to four or six would increase the maximum range of an BGV for a given glide speed and therefore help to reduce the amount of energy needed to reach a given range. This could reduce the mass of air-launched BGVs and could allow HCMs to carry less fuel for a given range. For many applications, simply using a booster large enough to achieve the desired range is likely preferable to the difficult task of increasing range by increasing glider L/D.

However, while the waverider concept dates from the late 1950s it has proved difficult to turn into working vehicles with high *L/D*. As a result, *L/D* of future systems may increase slowly over current values.

As we show, the effects of realistic increases in *L/D* on militarily relevant capabilities of BGVs are generally minor.

Effects of Changing L/D and β

The dynamics of the vehicle during glide (velocity profile, range, and flight time) depend primarily on *L/D* and very weakly on *β* for a given initial glide speed *V* and vehicle mass *m*. This can be seen from Equation 18 in the main text and the definition of *L/D*, which give:

$$F_L = \frac{1}{2} C_L A \rho V^2 = \alpha(V) mg \quad (B1)$$

$$F_D = \frac{1}{2} C_D A \rho V^2 = \frac{\alpha(V) mg}{L/D} \quad (B2)$$

where $\alpha(V) = 1 - (V/V_e)^2$, $V_e = [g(R_e+h)]^{0.5} \sim 8$ km/s for the altitudes of interest here, and R_e is the Earth radius.

These equations show that the forces acting on the vehicle during glide only depend on *β* through the small effect that the equilibrium glide altitude, which depends on *β* (Equation B3), has on

$\alpha(V)$ and g. In particular, the glide altitude h enters the force equations through g and V_e in the combination $R_e + h$, where R_e is the radius of the Earth.

As a result, changing β will change the drag at a given altitude but also change the glide altitude so that the vehicle feels essentially the same drag force. This implies that Acton's fitting to the test data of the HTV-2 constrained the value of L/D much more tightly than the value of β.[6] But since the glide dynamics depend only weakly on β, uncertainties in the value of β have little effect on the BGV dynamics analysis discussed in this paper and in Paper 1; changing β will affect the heating, as we discuss below.

Equation 23 in the main text shows that the range of a BGV increases with L/D. However, since the range depends roughly on the square of the glide speed V_g for the speeds considered here, that range increase could alternately be achieved by a small increase in V_g.

Heating of HGVs during the glide phase, which is a key issue for their development, depends on both L/D and β, and we next consider that dependence.

The glide altitude h can be determined from the density at the glide altitude, which from Equation B1 depends on the lift coefficient and can be written:

$$\rho(h) = \frac{2\alpha g\beta}{L/_D \; V^2} \qquad (B3)$$

The change in the vehicle's kinetic energy due to drag, which shows up as energy transfer to the air, depends on L/D but only very weakly on β. In particular, the rate of change of kinetic energy (KE) (ignoring the small change in potential energy during glide) equals the drag force times V, and using Equation B2 is:

$$\frac{dKE}{dt} = F_D V = \frac{\alpha mgV}{L/_D} \qquad (B4)$$

Ignoring the minor velocity dependence of $\alpha = (1\text{-}V^2/V_e^2)$ for speeds less than about Mach 12, this gives:

$$\Delta KE = \frac{\alpha mg}{L/_D} \int V dt = \frac{\alpha mg}{L/_D} r_G \qquad (B5)$$

so that the energy lost by the vehicle for a given glide range is inversely proportional to L/D. However, since the glide range for a BGV starting at V_g and ending at V_f is proportional to L/D, the total energy loss of the vehicle in that case is independent of L/D and depends only on the speeds at the start and end of glide, as expected:

$$\Delta KE = \frac{\alpha mg}{L/_D} r_G = \frac{m}{2}\left(V_g^2 - V_f^2\right) \qquad (B6)$$

where the last equality uses Equation D20 for the glide distance $r_G(V_g, V_f)$.[7]

Only a fraction of the energy lost by the BGV, however, is transferred from the air to the vehicle and results in heating of the body. A commonly used measure of the energy transfer to the vehicle is $dq/dt = \rho V^3$ (note that the empirical heating equations used in Paper 1 depend roughly on ρV^3) where q is the energy absorbed per area. Equation B3 gives:

$$\frac{dq}{dt} = \rho V^3 = \frac{2\alpha g V \beta}{L/D} \qquad (B7)$$

Unlike Equation B4, this quantity depends on β because the fraction of energy transferred from the air to the vehicle depends on the atmospheric density around the body, and the density at the glide altitude depends on β. Unlike the dynamics of the vehicle, the heating therefore depends on both β and L/D.

Since the vehicle's surface temperature T is proportional to the fourth root of dq/dt from the Stefan-Boltzmann law, the body temperature changes slowly with $\beta/(L/D)$.[8] Numerical calculations using the methods described in Paper 1 show that T is roughly proportional to $[\beta/(L/D)]^a$, where a = 1/7 to 1/5 for speeds below Mach 12, confirming that T varies only slowly with $\beta/(L/D)$.

For example, decreasing $\beta/(L/D)$ by a factor two, which would correspond, e.g., to increasing L/D from the HTV-2 value 2.6 to 5.2 (at constant β), would only reduce a glider's surface temperature by about 10%.

Moreover, if the vehicle takes advantage of the longer glide range that is possible with higher L/D, then the total energy absorbed by the vehicle would depend on β but not L/D. Ignoring the minor velocity dependence of α for speeds less than about Mach 12, one finds:

$$q = \frac{2\alpha g \beta}{L/D} \int V dt = \frac{2\alpha g \beta}{L/D} r_G = \beta\left(V_g^2 - V_f^2\right) \qquad (B8)$$

where r_G is the glide distance of the BGV starting at V_g and ending at V_f, which is proportional to L/D (Equation D20). The fact that q is proportional to β may be surprising since it means the energy absorbed decreases with a larger drag coefficient, but this is essentially the reason that early heat shields for spacecraft and reentry vehicles were blunt, which allowed these vehicles to slow at altitudes where atmospheric density was low.

For a given L/D and β, an effective way of limiting the heat load to a BGV is to limit its speed (which decreases the heat transfer rate) and/or to shorten its range (which reduces the duration of heating). This appears to be the current U.S. approach, since it is focusing on gliders with speeds below about Mach 12 and ranges of only up to a couple thousand kilometers, rather than long-range vehicles like the HTV-2. Reduced heating of a BGV would also decrease its infrared radiant intensity and therefore its visibility to IR sensors, such as SBIRS.

Effect of Varying L/D on Range and Flight-Time Calculations

Given the importance of the parameter L/D in determining the dynamics of a BGV, we illustrate how variations in L/D affect the results for range and flight time calculated in the main text.

Figures B1 and B2 show how the total mass and flight time versus range of a BGV vary with *L*/*D* for the Mach 9 case. *L*/*D* = 2.6 is the value estimated for the U.S. HTV-2 vehicle, while *L*/*D* = 2.2 is an estimate for the conical Common Hyper Glide Body (C-HGB) the United States is developing, as discussed in the main text.

These figures show that increasing *L*/*D* increases the maximum range that a BGV of a given total mass can reach, or alternately, reduces the total mass needed to reach a given range. However, because a lower value of *L*/*D* requires a vehicle to have a higher burnout speed to reach a given range, Figure B2 shows that *L*/*D* has little effect on the flight time to reach a given range.

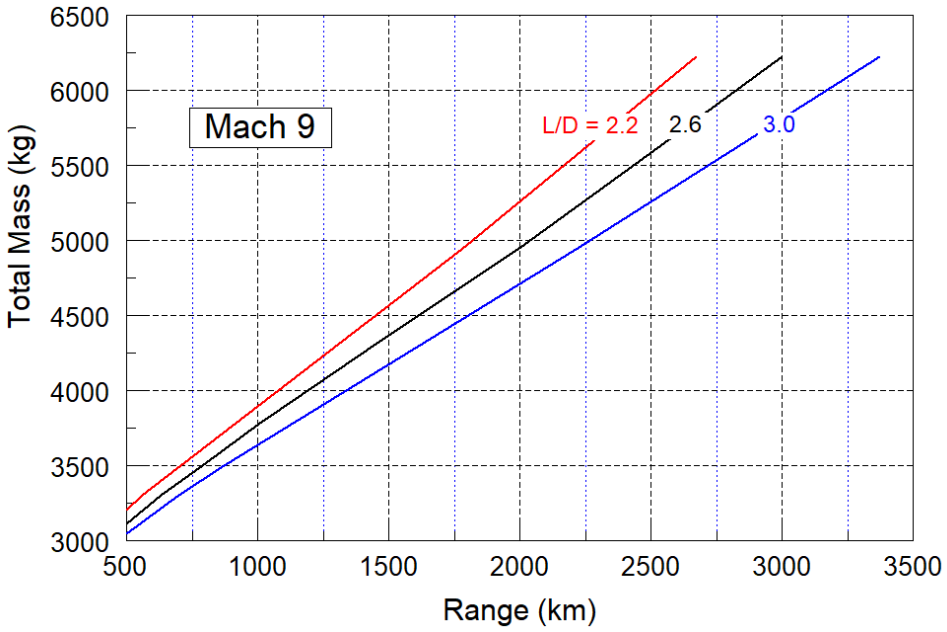

Figure B1: Total mass required for a BGV to reach a given range for different values of *L/D,* for the case in which the BGV dives when its glide speed slows to Mach 9. The BGV mass is 700 kg.

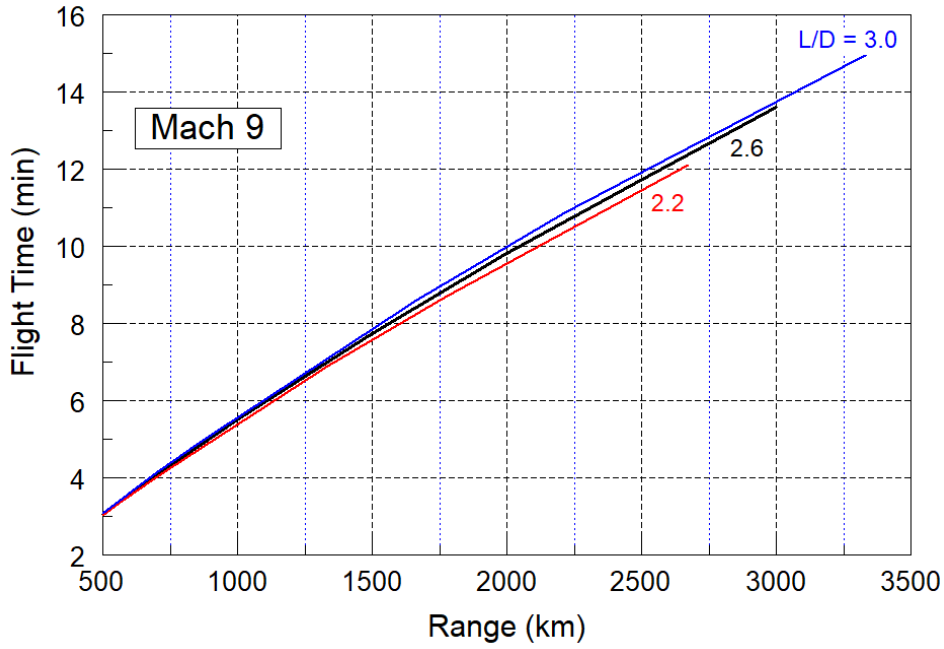

Figure B2: Flight time of a BGV to reach a given range for different values of *L/D,* for the case in which the BGV dives when its glide speed slows to Mach 9. These curves show the results for weapons up to 6,200 kg total mass, as in Figure B1. The BGV mass is 700 kg.

Appendix C: The Role of New Space-Based Sensors

The United States is developing space-based sensors to detect and track BGVs over much larger areas than ground-based radars and with better resolution than SBIRS. The proposed Hypersonic and Ballistic Tracking Space Sensor (HBTSS) system, for example, would include a constellation of many hundreds of satellites in low Earth orbit in addition to satellites at higher altitudes.[9] Such a tracking system could be useful as part of a longer-range defense system in the future.

Deploying and maintaining such a system, however, would be difficult and expensive. Moreover, since ground-based radars should be capable of detecting BGVs of the type considered here with sufficient range for interceptors to engage them, the most important step in improving current defenses against BGVs appears to be developing more capable interceptors, rather than developing new sensors.

This view is reinforced by an animation released by the Missile Defense Agency (MDA) that shows Aegis SM-6 interceptors and the proposed Glide-Phase Interceptor (GPI) engaging BGVs that are attacking U.S. ships.[10] The video indicates that HBTSS would not play a crucial role in the defense.

HBTSS is intended to provide sufficiently high-quality track data to allow the launch of interceptors before the BGV is within the range of the defense system's radar—so-called "engage-on-remote." However, the MDA video shows that engage-on-remote is not needed.

Instead, the video shows that forward-based radars on ships surrounding a carrier could detect and track a BGV earlier than a radar located near the carrier, allowing interceptor launch before the BGV was within the range of that second radar—a situation called "launch-on-remote." While not shown, the defense may be able to execute engage-on-remote using the information from the forward-based radar.

The video also shows that an interceptor could engage a BGV even when launched after the target was detected by the interceptor's co-located radar—a situation called "cued-organic-defense." This again suggests that HBTSS could increase the area defended by interceptors but is not required to protect ships.

Appendix D: Derivation of Glide Phase Equations

To model the glide phase, we first derive simple equations that can be used for low speeds and short ranges, which are useful for understanding the physics. We then derive equations that apply more generally.

During the glide phase, the drag force on the vehicle is:

$$F_D = \frac{1}{2} C_D A \rho V^2 = \frac{\rho}{2\beta} m V^2 \qquad (D1)$$

where ρ is the atmospheric density, $\beta = m/C_D A$ is the ballistic coefficient. The equations of motion show the lift force equals the total weight mg of the vehicle reduced by an inertial term due to its flight over a spherical Earth:

$$F_L = \left(1 - \frac{V^2}{V_e^2}\right) mg \equiv \alpha(V) mg \qquad (D2)$$

Here $V_e = [g(R_e+h)]^{0.5} \sim 8$ km/s for the altitudes of interest here, where R_e is the Earth radius. The function $\alpha(V)$ includes the inertial (centrifugal) effects at high speed. Since $F_L = (L/D)F_D$, Equations D1 and D2 can be solved for the equilibrium glide altitude h of the vehicle at speed V, where h corresponds to the atmospheric density satisfying:

$$\rho(h) = \frac{2\alpha g \beta}{L/_D \; V^2} = \frac{2\hat{g}\beta}{V^2} \qquad (D3)$$

Here

$$\hat{g} \equiv \frac{\alpha g}{L/_D} \qquad (D4)$$

plays the role of a reduced value of the gravitational constant in the presence of lift and inertial effects. Using Equation D3, F_D can be written:

$$F_D = \frac{\alpha m g}{L/_D} \equiv m\hat{g} \qquad (D5)$$

The function α varies by less than 10% as V changes from Mach 5 to Mach 10. As a result, for low speeds and short ranges, one can get useful approximations by assuming $\hat{g}$ and F_D are constant and estimating the glide velocity, time, and range (r) during glide by the Newtonian formulas:

$$V(t) = V_g - \hat{g}t \qquad (D6)$$

$$r(t) = V_g t - \frac{1}{2}\hat{g}t^2 \qquad (D7)$$

where V_g is the speed at the beginning of glide. These equations can be used to calculate the time t_G it takes to glide a distance r_G starting at a speed V_g:

$$t_G(r_G) = \frac{V_1}{\hat{g}}\left[1 - \left(1 - 2\hat{g}r_G/V_g^2\right)^{1/2}\right] \qquad (D8)$$

and the speed of the BGV after gliding a distance r_G:

$$V(r_G) = V_g\left(1 - 2\hat{g}r_G/V_g^2\right)^{1/2} \qquad (D9)$$

If glide begins with speed V_g and ends with V_f, then:

$$r_G(V_g, V_f) = \frac{V_g^2 - V_f^2}{2\hat{g}} = \frac{L}{D}\frac{\left(V_g^2 - V_f^2\right)}{2\alpha_g g} \qquad (D10)$$

and from Equation D6:

$$t_G(V_g, V_f) = \frac{V_g - V_f}{\hat{g}} = \frac{L}{D}\frac{\left(V_g - V_f\right)}{\alpha_g g} \qquad (D11)$$

Equations D10 and D11 can be improved by using the average value of $\alpha(V)$ over the glide phase, since V_f is known in this case. Numerical calculations integrating the full equations of motion show that these expressions are good approximations for speeds below Mach 10 to 12.

We next derive more general expressions that include the variation of F_D with V and that are accurate for higher speeds and longer ranges. Ignoring the very small change in potential energy of the BGV as its altitude changes during glide, the change in kinetic energy during glide equals the work done by drag:

$$d\left(\frac{mV^2}{2}\right) = -F_D dr = -\frac{mg}{L/D}\left(1 - \frac{V^2}{V_e^2}\right)dr \qquad (D12)$$

where the second equality uses Equation D5. This can be put in the form:

$$\int \frac{d(V^2)}{1 - \frac{V^2}{V_e^2}} = -\frac{2g}{L/D}\int dr \qquad (D13)$$

which can be integrated to give Equation 22 in the main text, and reduces to Equation D9 when r_G is short enough that the argument of the exponent is small (recall that $V_e^2/g = (R_e + h) \sim 6{,}400$ km).

Equation 23 gives the glide range of a BGV starting at V_g and ending at V_f, which is a more accurate version of Equation D10.

Equation 22 for $V(r)$ can also give the flight time during glide over a distance r_G with starting speed V_g, by integrating over $dt = dr/V(r)$:

$$t_G = \int dt = \int \frac{dr}{V(r)} = \frac{1}{V_e}\int \left[1 - \alpha_g \exp\left(\frac{2gr_G}{L/D\, V_e^2}\right)\right]^{-1/2} dr \qquad (D14)$$

Using a change of variable $s = \alpha_g^{1/2} \exp[g r_G/(L/D\ V_e^2)]$ this can be integrated to give Equation 24 in the text. Equation 25, which gives the time duration of glide starting at V_g and ending at V_f, is a more accurate version of Equation D11.

---

[1] Cameron L. Tracy and David Wright, "Modelling the Performance of Hypersonic Boost-Glide Missiles," *Science and Global Security* 28 (2021): 135–170, http://scienceandglobalsecurity.org/archive/sgs28tracy.pdf.

[2] Numerically integrating Equations (4) and (5) in our original equations simply adds up length increments at each time step in the local range and cross-range directions. We define angles Ψ and Ω by dividing those lengths by R_e, but those angles do not appear in the Equations (1), (2), (3), or (6). They can be visualized as shown in Figure B1.

[3] "Spherical Trigonometry," Wikipedia, https://en.wikipedia.org/wiki/Spherical_trigonometry.

[4] "Spherical Trigonometry," Wikipedia.

[5] See, eg, John D. Anderson, Jr., *Introduction to Flight, Eighth edition* (Reston, VA: American Institute of Aeronautics and Astronautics, 2016): 839.

[6] James M. Acton, "Hypersonic Boost-Glide Weapons," *Science and Global Security* 23 (2015): 191–219, http://scienceandglobalsecurity.org/archive/sgs23acton.pdf, estimates β = 13,000 kg/m^2 for the HTV-2 from its test data. Using CFD calculations, Graham V. Candler and Ivett A. Leyva, "Computational Fluid Dynamics Analysis of the Infrared Emission from a Generic Hypersonic Glide Vehicle," *Science and Global Security,* 7 December 2022, https://doi.org/10.1080/08929882.2022.2145777, estimate a value of β = 4680 kg/m^2 for a vehicle like the HTV-2.

[7] This result also comes from including the V dependence of α and integrating the more exact Equations 22 and 23.

[8] Encyclopedia Britannica, "Stefan-Boltzmann Law," https://www.britannica.com/science/Stefan-Boltzmann-law.

[9] "Hypersonic and Ballistic Tracking Space Sensor (HBTSS)," *Missile Defense Advocacy Alliance* (2 July 2020), https://missiledefenseadvocacy.org/defense-systems/hypersonic-and-ballistic-tracking-space-sensor-hbtss/.

[10] Missile Defense Agency (MDA), "MDA Hypersonic Concept," Defense Visual Information Distribution Service (6 June 2021), https://www.dvidshub.net/video/801628/mda-hypersonic-concept; Theresa Hitchens, "Next Budget Will Limit Glide Phase Interceptor Contractors: MDA Head," *Breaking Defense,* 12 August 2021, https://breakingdefense.com/2021/08/next-budget-will-limit-glide-phase-interceptor-contractors-mda-head/.